Theoret. Chim. Acta (Berl.) 60, 159–172 (1981)

THEORETICA CHIMICA ACTA

Ab initio Calculation of the Band Structure of some Boron Polymers

David R. Armstrong

Department of Pure and Applied Chemistry, University of Strathclyde, Glasgow G1 1XL, Scotland, U.K.

Ab initio calculations using a STO-3*G* basis set have been performed on the polymer systems $(HBX)_n$ where X = Be, BH, CH_2, NH, and O. Energy band diagrams and accompanying density-of-states plots have been obtained. The highest filled orbital of $(HBNH)_n$ and $(HBO)_n$ occurs at the *X*-point and possesses π character while the σ-framework orbital at the *X*-point is the highest filled level for $(HBBe)_n$, $(HBBH)_n$, and $(HBCH_2)_n$. The conduction band for all five species has π symmetry and the band gap of the $(HBX)_n$ species increases in the order X = Be < BH < NH < O < CH_2. An estimate of the energy of polymerisation of the $(HBX)_n$ systems suggests that HBNH is particularly stabilised by polymerisation. The electron distribution in $(HBBe)_n$ shows a σ – electron drift towards boron, while in the other four systems the net electron transfer is directed away from boron. There is significant π electron back-donation to boron in $(HBO)_n$ and $(HBNH)_n$.

Key words: Boron Polymers – *Ab initio* calculations – Band structure calculations.

1. Introduction

Boron forms a large number of high-molecular-weight compounds with many elements. In particular these involve bonds of boron with the first- and second-row non-metals. The high bond energy of these bonds indicates a comparable strength to the C—C bonds and this has led to great experimental effort to synthesise polymers based on these bonds. In order to aid these investigations we have computed the band structure and electron distribution of a series of

0040-5744/81/0060/0159/$02.80

simple polymers $(HBX)_n$ formed from the unsaturated boron monomers HB=X where X = Be, BH, CH_2, NH, and O.

2. Calculational Method

The calculations employed the *ab initio* formalism due to André [1]. The basis set consisted of the ubiquitous three contracted gaussian functions per Slater-type orbital [2]. All the orbital exponents were abstracted from the work of Clementi and Raimondi [3] except the Be 2*p* orbital exponent which was taken from previous calculations on BeH_2 [4]. The nearest-neighbour approximation which allows only the interactions between three adjacent unit cells to be incorporated in the SCF procedure was imposed on our calculational procedure. This limits the accuracy of the calculation of the total energy and thus a complete geometry optimisation of the unit cell (see Fig. 1) was considered unnecessary and unprofitable. However, optimisation of the BX framework bond-length, which is a parameter of considerable interest, was performed. Standard bond lengths extracted from the literature [5] were employed for the remaining bonds and the framework bond angles were set at 120°.

3. Results and Discussion

The electron band diagrams and electron distribution will be discussed initially and this will be followed by a summary of the general trends displayed by the five polymer systems.

3.1. The Electronic Structure of $(HBBe)_n$

There have been no previous calculations on boron-beryllium polymers, although computations on the electronic structure of $(BH_2)_n$ and $(BeH_2)_n$ [4] and the monomer HBBe [6] have been reported. The electron band structure of $(HBBe)_n$ is presented in Fig. 2c. There are five occupied bands of $(HBBe)_n$, the two low energy core bands 1 and 2 which are not shown in the diagram lie at −7.56 a.u. and −4.63 a.u. Bands 3 and 4 are flat, indicative of localised bonding, while band 5 is

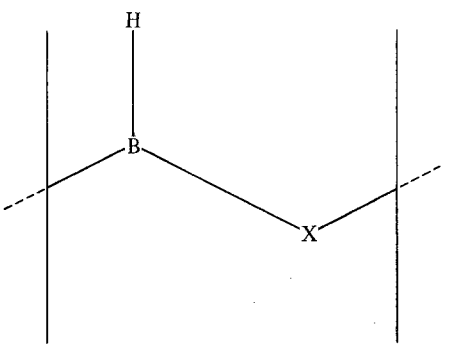

X = Be, BH, CH_2, NH, and O.

Fig. 1. The unit cell of HBX

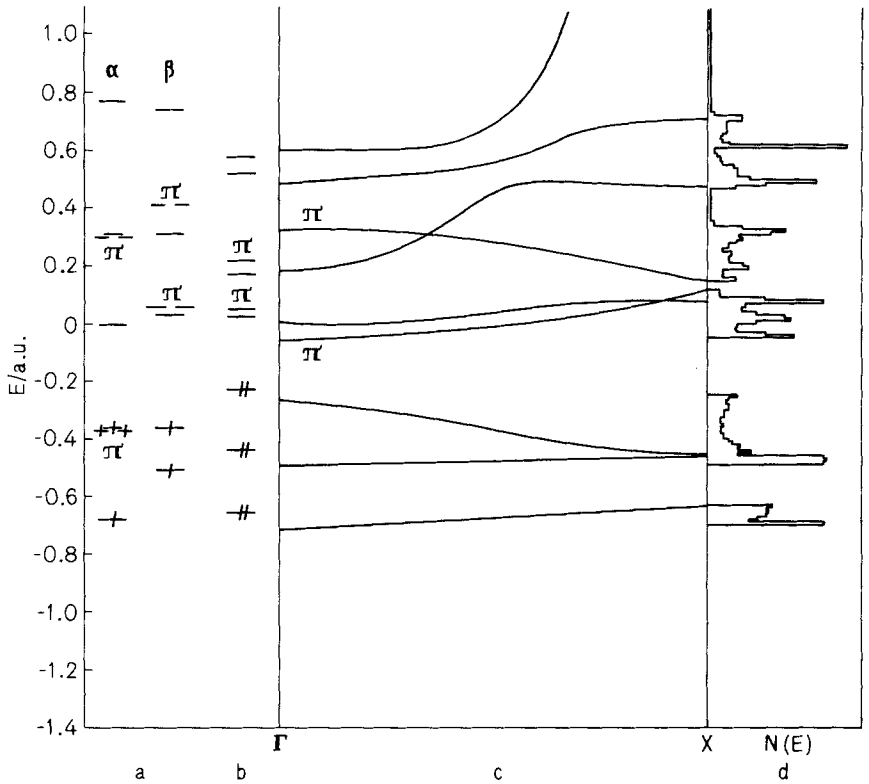

Fig. 2. **a** The energy levels of HBBe in its optimum geometry, **b** the energy levels of HBBe in a reorganised geometry, **c** the energy band diagram of $(HBBe)_n$, and **d** the density of states of $(HBBe)_n$

curved with a width of 5.3 eV. Inspection of the eigenvectors reveals that at the Γ-point, band 3 is largely composed of B 2*s* and H 1*s* orbitals and this composition is only slightly modified by the increased participation of the Be $2p_x$ orbital as the k_x value increases to 0.5. Band 4 represents the B—H bonding orbital with the H 1*s* and B $2p_y$ orbitals as the main components of the interaction. The valence band represents framework boron-beryllium bonding. At the Γ-point this molecular orbital is almost exclusively formed from a bonding combination of B $2p_x$ and Be $2p_x$ orbitals while at the *X*-point there is a substantial contribution from the Be 2*s* orbital and this is associated with the increased stability of this level. Hence, the highest filled level of the polymer occurs at the Γ-point with an ionisation energy of 7.36 eV. The lowest vacant level also occurs at the Γ-point and so the lowest band gap is direct, measuring 5.79 eV. Thus, $(HBBe)_n$ is predicted to have semi-conducting properties. The conduction band is of π symmetry. At the Γ-point there is almost equal participation of the π orbitals of B and Be, while at the *X*-point there is a greater contribution from the *B* π orbital and a consequent increase in energy. A density-of-states histogram of $(HBBe)_n$ presented in Fig. 2d predicts that there will be two main peaks in the

photoelectron spectrum of $(HBBe)_n$. One will be centred at 19.0 eV while the higher energy band will be present at 13.1 eV.

The molecular-orbital energies of the monomer HBBe are presented in Fig. 2a, b. The energy levels of HBBe in its most stable geometry [6] are displayed in Fig. 2a while the eigenvalues of HBBe, with a geometry identical to that present in a unit cell of the polymer, are plotted in Fig. 2b. The triplet state of the linear monomer is the more stable spin state and, as expected, possesses energy levels which are more stable than those of the reorganised monomer. Comparison of Fig. 2b,c clearly demonstrates the effect of polymerisation upon the energy levels as all three valence levels become more stabilised upon association. This is especially true of the highest filled molecular orbitals of the distorted monomer and this orbital can be correlated with a π orbital of the linear HBBe moiety.

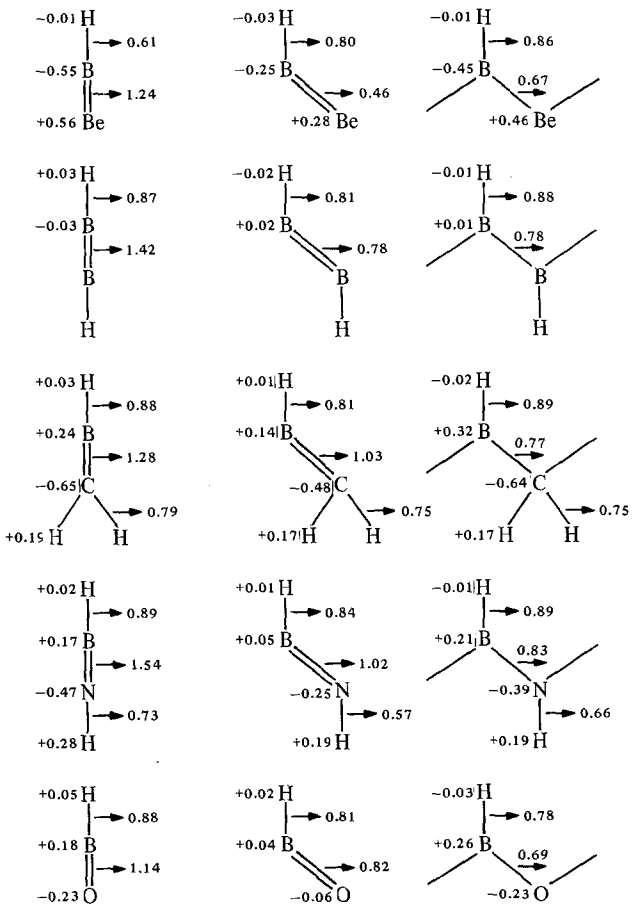

Fig. 3. The electron distribution of HBX and $(HBX)_n$ for X=Be, BH, CH_2, NH, and O

The electron distribution of HBBe and $(HBBe)_n$ is presented in Fig. 3. There is an electron flow from Be to the HB portion for all three species considered. In the polymer the valence electron distribution of beryllium is $(2s^{0.69}2p_x^{0.78}2p_y^{0.07})$ illustrating the low participation of the Be $2p_y$ orbital in the bonding. The donated electron density (0.46) is found in the boron $2p_x$ (0.34) and $2s$ (0.12) orbitals. There is a more pronounced charge transfer in the linear monomer, while in the reorganised monomer the charge distribution is less polarised than in the polymer. The boron-beryllium bond overlap population is reduced by the reorganisation of the monomer. Upon polymerisation of HBBe the overlap population of this bond is increased with respect to the reorganised monomer. Although the overlap population is smaller than that of the monomer, there are now two framework bonds per HBBe unit, so the total boron-beryllium bond population of the polymer is greater than that of the monomer.

3.2. The Electronic Structure of $(HBBH)_n$

A polymeric compound of boron and hydrogen $(H_xB)_n$ where x is close to one has been isolated [7]. There has been no previous calculation on $(HBBH)_n$ in contrast to the detailed theoretical investigation [8] of the geometry of HBBH. The electronic structure of the related species $(H_2BBH_2)_n$ has been reported [4] and it was found that firstly, an alternating-bond model is more appropriate than a symmetric-bond representation of $(H_2BBH_2)_n$ and secondly, the monomeric species is more stable than the polymeric form of $(H_2BBH_2)_n$. It as of interest to find if these two relationships were valid for $(HBBH)_n$.

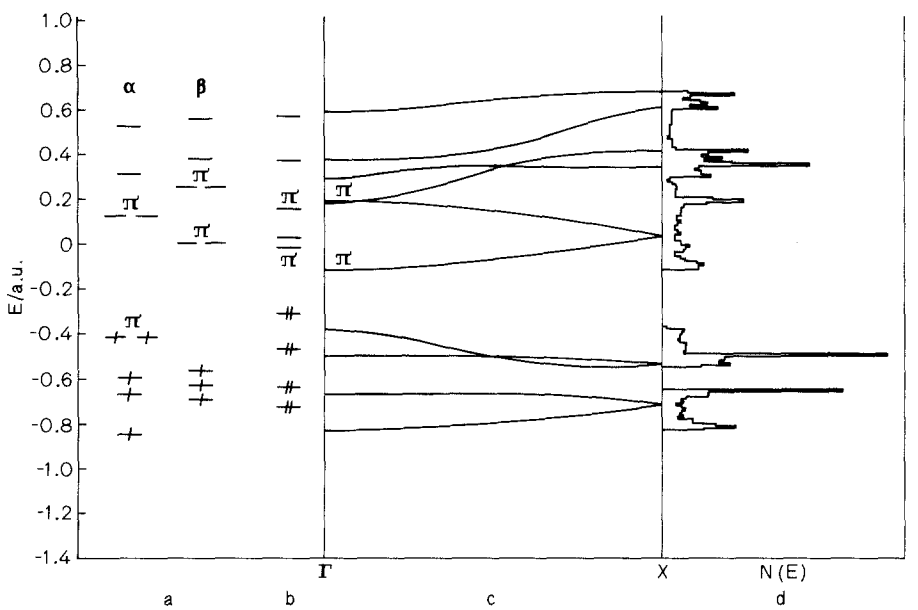

Fig. 4. a The energy levels of HBBH in its optimum geometry, **b** the energy levels of HBBH in a reorganised geometry, **c** the energy band diagram of $(HBBH)_n$, and **d** the density of states of $(HBBH)_n$

The electron-band structure of symmetric $(HBBH)_n$ is presented in Fig. 4. Two low-lying bands, not shown in the diagram, occur at −7.66 a.u. The next four filled valence bands (3–6) are of σ-symmetry and lie between −22.1 and −10.4 eV. Band 3 is largely composed of B $2s$ and H $1s$ orbitals at the Γ-point and is modified by the increase in the B $2p_x$ orbital participation as the X-point is approached. The fourth band is similar in composition to the third band, except for the substantial presence of the B $2p_y$ orbital at the Γ-point which diminishes as k_x moves towards 0.5. The fifth band consists of H s and B $2p_x$ orbital interactions at $k_x = 0$ and these are joined by increased B $2p_x$ orbital contributions as the X-point is approached. The sixth band at the Γ-point is strictly a B $2p_x$–B $2p_x$ interaction which becomes modified as k_x increases through increased bonding of the H s and B $2p_y$ orbitals. The highest filled level of $(HBBH)_n$ occurs in this band at the Γ-point and has an energy of −10.4 eV. The lowest vacant orbital which has π-symmetry is also present at the Γ-point and the resulting direct band gap spans 7.5 eV. The non-degeneracy of the high-energy virtual orbitals at X highlights the inadequacy of the nearest-neighbour approximation. The density-of-states plot of $(HBBH)_n$ shows three main peaks at −22.3, −17.7, and −13.6 eV. The filled bands span two regions of 4.9 eV, while the conduction bands are spread over 21.5 eV.

The orbital energies of monomeric HBBH are plotted in Fig. 4a, b. The singly-filled π orbitals of the linear molecule split upon reorganisation into a doubly filled σ orbital and a vacant π orbital. Comparison of the band plot of $(HBBH)_n$ with energy levels of reorganised HBBH indicates a large stabilisation of this σ-orbital upon polymerisation.

The electron distribution of the monomeric and polymeric structures of HBBH is displayed in Fig. 3. There is only a small polarisation of charge between the boron and hydrogen. The valence electron distribution for boron in the polymer is $(2s^{1.09}2px^{0.95}2py^{0.95})$ which is close to the expected sp^2 hybrid electron distribution. The B—B overlap population is highest for the optimum geometry of HBBH and this has been greatly reduced upon geometry reorganisation and polymerisation. The total B—B overlap population per unit cell (1.558), however, exceeds that of the monomer (1.416).

Further calculations on $(HBBH)_n$ reveal that the symmetric-bond model of $(HBBH)_n$ is found to be more stable than an alternating-bond model. The energy of the former model is found to be more stable than the monomer and thus a polymeric boron hydride is predicted to be based on a $(HBBH)_n$ system.

3.3. The Electronic Structure of $(HBCH_2)_n$

There have been no previous calculations on boron–carbon polymers. Pople et al. [8] have performed a thorough theoretical investigation on some simple boron–carbon molecules and have obtained the optimum geometry of $HBCH_2$.

The band structure of $(HBCH_2)_n$ is presented in Fig. 5c. There are two low-lying core bands centred at −11.2 a.u. and −7.67 a.u. and five filled valence bands.

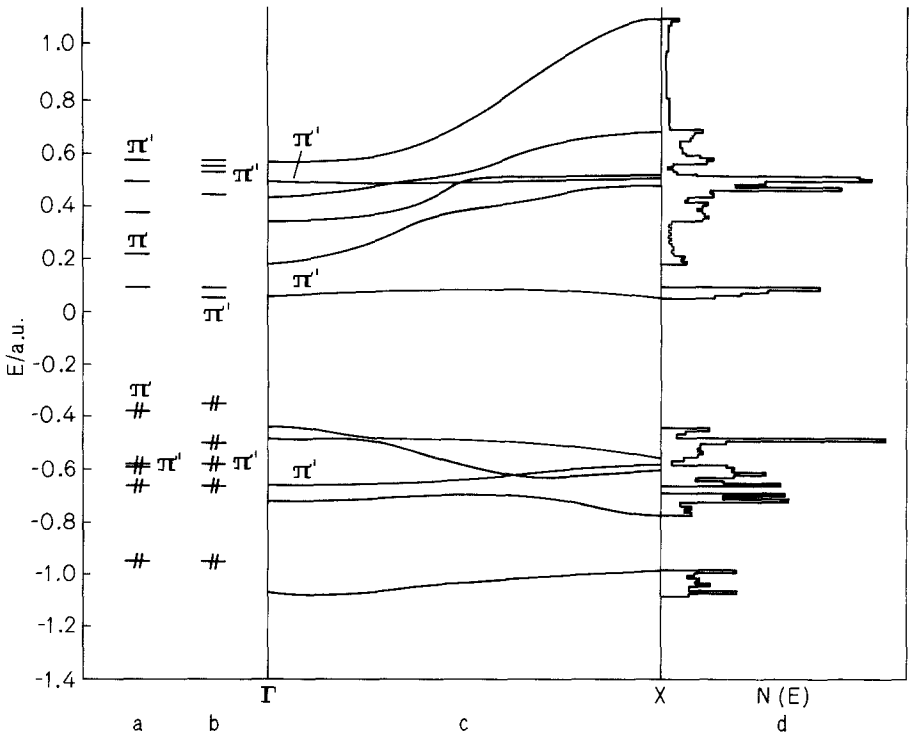

Fig. 5. **a** The energy levels of $HBCH_2$ in its optimum geometry, **b** the energy levels of $HBCH_2$ in a reorganised geometry, **c** the energy band diagram of $(HBCH_2)_n$, and **d** the density of states of $(HBCH_2)_n$. (π' represents hyperconjugative bonding)

Band 3 possesses a large C $2s$ orbital component, a small B $2s$ orbital contribution, and a B $2p_x$ orbital value which varies directly with k_x. Bands 4 and 6 can be associated at the Γ-point with carbon–hydrogen and boron–hydrogen bonding orbitals. Band 5 has π' symmetry and this is localised about the CH_2 portion with a small boron $2p_z$ orbital contribution which diminishes as the X-point is approached. At $k_x=0$, band 7 consists of the framework B $2p_x$ − C $2p_x$ interactions which are joined by B $2p_y$ and C $2p_y$ interactions as k_x increases. The lowest vacant band has π' symmetry and is very flat due to the localised nature of the bonding centred on boron with only a small contribution from the CH_2 portion. The lowest vacant and highest filled levels occur at the Γ-point resulting in a band gap of 13.6 eV and a first ionisation potential of 11.9 eV. The density-of-states graph shows the three main regions of the valence orbital energies. There is an area at −27.2 eV spanning 2.7 eV, a second region of 2.4 eV with a peak at −19.0 eV and a broad area of 5.7 eV possessing peaks at −18.0, −16.9, and −13.1 eV.

The orbital energy plots of $HBCH_2$ are presented in Fig. 5a, b. The optimum geometry of $HBCH_2$ posseses two planes of symmetry so π bonding and hyperconjugative (π') bonding can take place. When the monomer is distorted to

the reorganised form appropriate for polymerisation, the symmetry of the former becomes σ-type. The two highest filled molecular orbitals of the monomer are particularly destabilised by geometry reorganisation. This is not surprising as both orbitals are concerned with B—C bonding and have B—C overlap populations of 0.22 (m.o. 6) and 0.42 (m.o. 5). Comparison of the band diagram of Fig. 5c with the orbital energies of 5b confirms that a large stabilisation of the highest filled m.o.'s occurs upon polymerisation of $(HBCH_2)_n$.

The electron distribution of $HBCH_2$ and $(HBCH_2)_n$ is displayed in Fig. 3. The high negative charge on the carbon in the polymer is due to large sigma electron drift from the boron (0.39) and from the hydrogen atoms (0.34) combined with a small hyperconjugative π electron back transfer to the boron $2p_z$ orbital (0.09). The main beneficiary of the electron donation is the C $2s$ orbital while the B $2p$ orbitals are the principal contributing orbitals. The total B—C overlap population upon polymerisation is 1.544 and, compared with the value of the monomer, 1.284, produces a gain of 0.260 which is the highest increase in this series of HBX species.

3.4. The Electronic Structure of $(HBNH)_n$

Boron–nitrogen compounds have frequently attracted the attention of the theoretical chemist and iminoborane (HBNH) is no exception [8–10]. In particular, the important property of association of boron–nitrogen compounds has been probed by investigations into dimerisation [9, 10] and trimerisation [9] of HBNH. The gain in stabilisation energy by these processes amounted to 63 and 194 kcal/mole [9] respectively. The electronic structure of the polymer $(HBHN)_n$ has been examined previously by *ab initio* [11] and CNDO calculational schemes [12] and complements this study.

The band structure of $(HBNH)_n$ is displayed in Fig. 6c. The topography of the bands is similar to those presented in Ref. [11] where a smaller basis set was used in the calculation. The two low-lying bands associated with the boron $1s$ and nitrogen $1s$ orbitals are situated at -7.69 a.u. and -15.50 a.u., respectively. Band 3 has a large contribution from the nitrogen $2s$ orbital plus minor contributions from the boron $2s$ and $2p_x$ orbitals which decrease and increase, respectively, as k_x increases from Γ to X. At Γ, bands 4 and 5 can be described as the N—H and B—H bonding bands, respectively, while band 7 contains the B—N framework bonding contributions. As k_x increases to 0.5 the various contributions become scrambled and at X, band 4 is a boron–nitrogen framework bonding orbital while bands 5 and 6 contain N—H and B—H bonding components. The sixth band at Γ is a π orbital which has a large contribution from the nitrogen $2p_z$ orbital. As k_x increases this contribution increases until, at X, there is only a minute contribution from the boron $2p_z$ orbital. The resulting destabilisation due to this decreased bonding participation of the boron π orbital from Γ to X is 4.4 eV. The lowest ionisation potential of $(HBNH)_n$ occurs from this band at X and is 10.6 eV. The first vacant band has π symmetry and its band width is 4.4 eV. The composition of the conduction band at Γ consists of almost equal antibonding

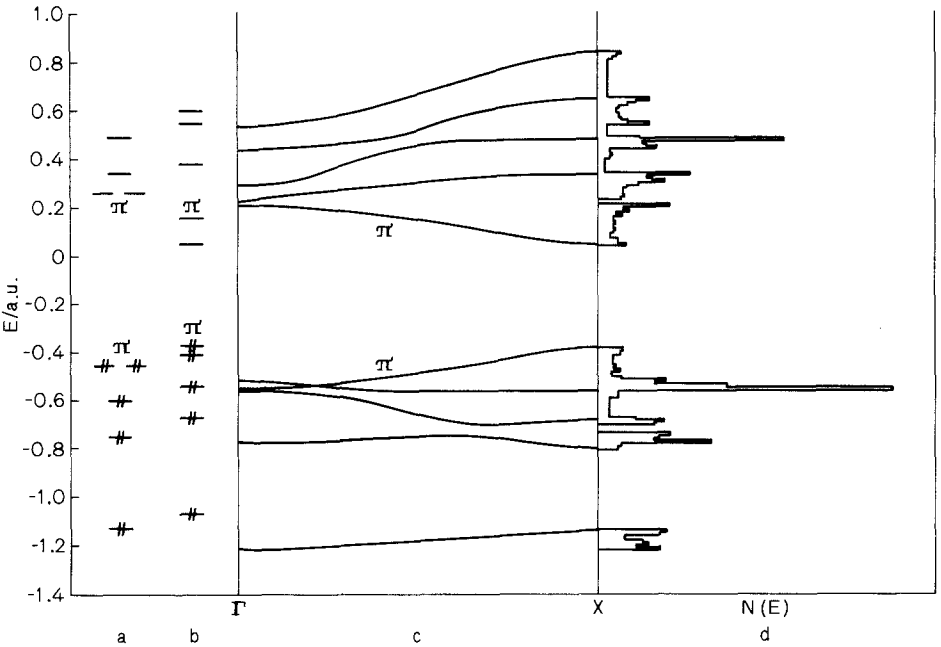

Fig. 6. **a** The energy levels of HBNH in its optimum geometry, **b** the energy levels of HBNH in a reorganised geometry, **c** the energy band diagram of $(HBNH)_n$, and **d** the density of states of $(HBNH)_n$

contributions from the boron and nitrogen $2p_z$ orbitals while at X the band is almost exclusively a boron $2p_z$ orbital. Increased antibonding contribution of the nitrogen $2p_z$ orbital produces increased destabilisation of the band. Hence the lowest vacant level of $(HBNH)_n$ occurs at X and the lowest band gap of $(HBNH)_n$ is direct and totals 11.9 eV. The direct transition will involve a charge transfer from the nitrogen $2p_z$ orbital to the boron $2p_z$ orbital. The density-of-states of $(HBNH)_n$ presented in Fig. 6d shows the three main valence band energy areas. The first two areas are 1.9 eV wide and are centred about −32.4 eV and −22.8 eV. The third region stretches over 9.1 eV and has two prominent peaks at −15.5 eV and −19.0 eV.

The orbital energies of linear and reorganised HBNH are plotted in Figs. 6a, b, respectively. The distortion of the linear molecule produces the expected destabilisation of the energy levels, while the formation of a polymer stabilises the levels. This is especially effective for the second-highest filled level of reorganised HBNH, which can be correlated with band 7 at Γ and band 4 at X and has a large nitrogen $2p_x$ orbital content.

The electron distribution of the various forms of HBNH is presented in Fig. 3. There is an overall electron drift from the B—H group to the N—H group of 0.20 electrons in $(HBNH)_n$. This comprises a dominating 0.65 σ-electron drift from the boron coupled with a back-donating π-electron shift of 0.45 electrons to the boron. The charges on the B—H and N—H groups in the linear monomer and polymer of HBNH are remarkably similar.

3.5. *The Electronic Structure of* $(HBO)_n$

There have been no previous calculations on the electronic structure of $(HBO)_n$ although calculations have been performed on boron–oxygen molecules [8, 13] including the monomer HBO [8]. A related study [14] has examined by a CNDO-based method the band structures of $(B(OH)O)_n$, $(B(OM)O)_n$ where M=Li and Na, and $(B_2O_3)_n$ in order to rationalise the principal mechanism of absorption in borate glasses. It will be of interest to find if the optical transitions in $(HBO)_n$ are of the same type and magnitude.

The valence-electron band structure of $(HBO)_n$ is presented in Fig. 7c. The low-lying $1s$ core bands are found at −20.46 a.u. and −7.73 a.u. Band 3 is a low-energy band which is largely composed of the oxygen $2s$ orbital. The small increase in energy of the band as k_x increases from 0.0 to 0.5 is matched by an added contribution of the boron $2p_x$ orbital. The fourth band at Γ contains B—H bonding interactions plus oxygen $2s$ and $2p_y$ orbital contributions. As k_x increases, the oxygen $2p_x$ orbital component increases, so that from $k_x = 0.3$ to 0.5 the band is the framework bonding orbital consisting largely of a B $2s$–O $2p_x$ interaction. The latter portion of the band can be linked with the sixth band at Γ

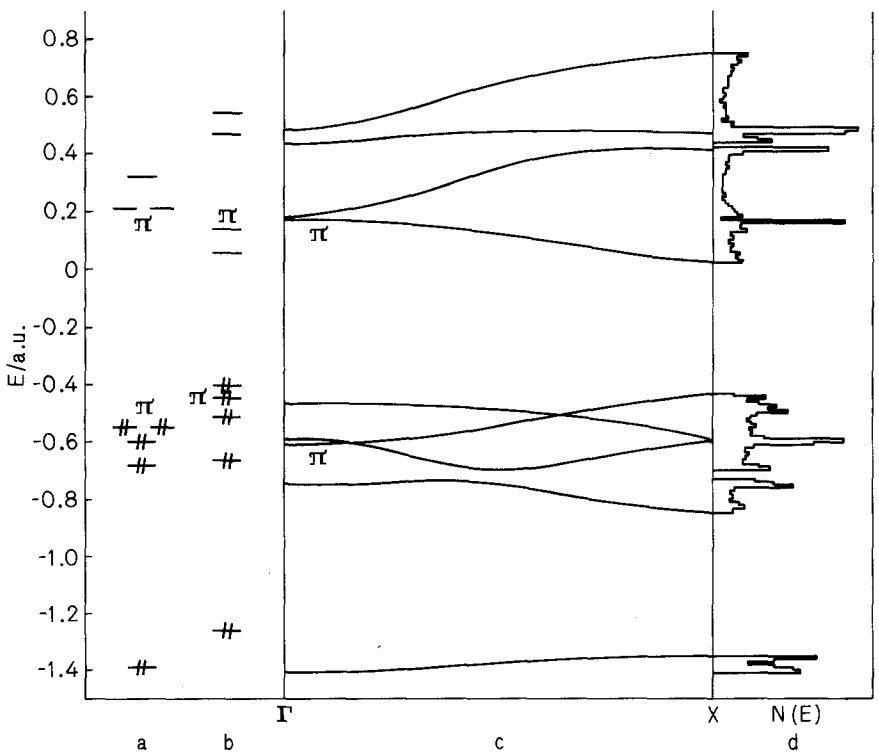

Fig. 7. **a** The energy levels of HBO in its optimum geometry, **b** the energy levels of HBO in a reorganised geometry, **c** the energy band diagram of $(HBO)_n$, and **d** the density of states of $(HBO)_n$

which contains a B $2p_x$–O $2p_x$ framework bonding component only. An increase in the k_x value produces an increase in the O $2p_y$ orbital coefficient, so that at X the sixth band contains H s, B $2p_x$, B $2p_y$, and O $2p_y$ orbital contributions and is similar in character to that of band 4 at Γ. The seventh band at Γ is dominated by the orbital contributions from H s and O $2p_y$. This is modified when k_x is increased by the added presence of the B $2p_x$, B $2p_y$ and 0 $2p_x$ orbitals. The fifth band at Γ has π symmetry with a large orbital coefficient for oxygen (0.72). As k_x increases to 0.5, then this coefficient approaches 1.0 with a corresponding loss of π-bonding and a consequent increase in energy of 4.5 eV. The highest filled level of $(HBO)_n$ with an ionisation energy of 12.1 eV occurs at X and is a π orbital which is localised about the oxygen atom. The lowest vacant orbital is of π symmetry and possesses an almost equal antibonding mixture of B $2p_z$ and O $2p_z$ orbitals at Γ. The composition of the band becomes totally B $2p_z$ orbital at X with a consequent decrease in the orbital energy. Thus, the highest filled and lowest vacant levels occur at the X-point and they both possess π symmetry. The inter-band gap is 12.8 eV and the lowest energy transition has charge-transfer character involving an oxygen $2p\pi \rightarrow$ boron $2p\pi$ electron shift. This is similar in nature to the transition which was reported for $(HOBO)_n$. [14]

The density-of-states plot for $(HBO)_n$ gives three main valence band areas. The lowest energy band is narrow and stretches from −38.3 to −36.7 eV. The second region spans 6.5 eV with a peak at −20.7 eV. The highest energy band area which covers 14.7 eV has a high concentration of levels at −13.6 eV, −16.3 eV, and −18.8 eV.

The orbital energies of monomeric HBO are displayed in Fig. 7a, b and can be compared with the band energies of $(HBO)_n$. The now familiar features found in the earlier members of the series are present in $(HBO)_n$. The highest filled π orbital of linear HBO gives upon reorganisation two higher energy levels of π and σ symmetry. The latter forms the basis of the framework bonding of the polymer and there is the expected stabilisation of the energy levels when polymerisation occurs.

The electron distribution of polymeric HBO shows an expected net electron flow from boron to oxygen of 0.23 electrons. This is comprised of a dominating σ-electron drift to the oxygen of 0.68 electrons plus a back-bonding donation of 0.45 electrons to the boron π orbital.

3.6. General Trends

(i) Electronic Band Structure

The lowest valence band of $(HBX)_n$ becomes detached from the rest of the valence bands and moves to lower energy as X progresses from Be to O. The shape of this band remains constant throughout the series and it represents the energies of a localised orbital centred on the 2s orbital of the most electronegative atom. The most delocalised bands are the σ-framework orbital band and the π bands. The former decreases in energy from $\Gamma \rightarrow X$ due to increased participation

of the $2p_y$ orbitals of B and X producing a more direct bond between B and X. The energy of the lowest π orbital band increases from $\Gamma \rightarrow X$ due to a smaller involvement of the boron π orbital in π bonding. This band at X is the highest filled level for $(HBNH)_n$ and $(HBO)_n$ while the σ-framework orbital at Γ is the highest filled level for $(HBBe)_n$ and $(HBBH)_n$. The bands which represent the hydrogen–atom bonding are localised in nature and therefore are generally flat with a small decrease in energy from Γ to X. The lowest vacant band has π character for all five systems. For the first two species, $(HBBe)_n$ and $(HBBH)_n$ this is the lowest π orbital and so the energy of the band increases from Γ to X, while for the remaining three systems it is the second π orbital and the energy of the band decreases from Γ to X. The band gap, ionisation potential, and the boron $1s$ band energy value of the five systems are presented in Table 1. The largest band gap is present in $(HBCH_2)_n$, whilst the largest ionisation potential is found in $(HBO)_n$. The boron $1s$ orbital energy of the $(HBX)_n$ species decreases in energy as the electronegativity of X increases.

(ii) Energy of Polymerisation

The energy of polymerisation of $(HBX)_n$, defined simply as the difference in the total energies of the polymer per unit cell and the corresponding monomer, is listed in Table 2. Also included in the table is the reorganisation energy of $(HBX)_n$ which is the energy required to reorganise the geometry of the monomer from the optimum configuration to a conformation suitable for forming a polymer. $(HBNH)_n$ possesses the highest energy of polymerisation and this is 69–85 kcal/mole greater than that calculated for the other four systems. This finding parallels the variation in the overlap population of the B—X bond which has a maximum for $(HBNH)_n$ and underlines the importance of the property of association in the chemistry of B—N compounds. The reorganisation energy is highest for HBNH and HBO and this reflects the additional π component present in these B—X bonds which will be also weakened by reorganisation of the linear configuration of the monomer.

(iii) Electron Distribution

The electronic charge of the X moiety in $(HBX)_n$ is very similar to that present in the monomer HBX, although it is very different from that of the reorganised monomer. Boron carries a positive charge in all the $(HBX)_n$ systems except for

Table 1. The band gap, ionisation potential, and the boron $1s$ orbital energy of the $(HBX)_n$ species

	$(HBBe)_n$	$(HBBH)_n$	$(HBCH_2)_n$	$(HBNH)_n$	$(HBO)_n$
Band Gap (eV)	5.79	7.48	13.57	11.86	12.81
Ionisation Potential (eV)	7.36	10.40	11.88	10.61	12.05
Boron $1s$ Orbital Energy (a.u.)	−7.56	−7.66	−7.67	−7.69	−7.73

Table 2. Polymerisation energy (in kcal mole) of the HBX species

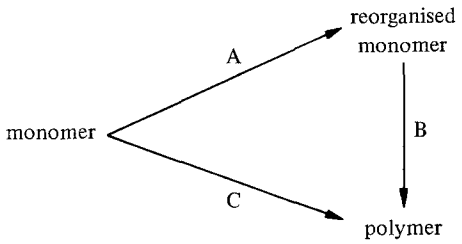

	A	B	C
HBBe	36.9	284.3	247.4
HBBH	41.3	298.7	257.4
$HBCH_2$	29.8	290.1	260.3
HBNH	57.5	389.9	332.3
HBO	63.2	326.6	263.4

$(HBBe)_n$. In $(HBCH_2)_n$, $(HBNH)_n$ and $(HBO)_n$ there is a large σ-electron drift from B to X and this is coupled with a π electron back-donation for $(HBO)_n$ and $(HBNH)_n$.

(iv) B—X Bond Distances

The optimised B—X distances of the $(HBX)_n$ polymers calculated within the nearest-neighbour approximation are presented in Table 3. Also included in this table are the optimised bond lengths [6, 8] of the monomeric compounds. The B—X bond lengths increase upon polymerisation, with the B—B bond length in $(HBBH)_n$ undergoing the largest increase. These bond-length increases reflect the change in bonding between boron and atom X from a formally double bond to a single bond.

Table 3. Optimised BX bond lengths of the $(HBX)_n$ species

	BX Bond Lengths (Å) of $(HBX)_n$	
	Monomer[a]	Polymer
HBBe	1.74	1.80
HBBH	1.43	1.88
$HBCH_2$	1.34	1.56
HBNH	1.20	1.53
HBO	1.18	1.48

[a] Taken from Refs. [6] and [8].

References

1. André, J. M.: Comp. Phys. Commun. **1**, 391 (1970)
2. Stewart, R. F.: J. Chem. Phys. **52**, 431 (1970)
3. Clementi, E., Raimondi, D. L.: J. Chem. Phys. **38**, 2686 (1963)
4. Armstrong, D. R., Jamieson, J., Perkins, P. G.: Theoret. Chim. Acta (Berl.) **51**, 163 (1979)
5. 'Interatomic Distances': J. Chem. Soc. Special Publication no. 11, London, 1958
6. Dill, J. D., Schleyer, P. v. R., Pople, J. A.: J. Am. Chem. Soc. **99**, 6159 (1977)
7. Koester, R.: Angew. Chem. **70**, 743 (1958)
8. Dill, J. D., Schleyer, P. v. R., Pople, J. A.: J. Am. Chem. Soc. **97**, 3402 (1975)
9. Armstrong, D. R., Clark, D. T.: Theoret. Chim. Acta (Berl) **24**, 307 (1972)
10. Baird, N. C., Datta, R. K.: Inorg. Chem. **11**, 17 (1972)
11. Armstrong, D. R., Jamieson, J., Perkins, P. G.: Theoret. Chim. Acta (Berl.) **49**, 55 (1978)
12. Armstrong, D. R., McAloon, B. J., Perkins, P. G.: J. Chem. Soc. Faraday II Trans. **69**, 968 (1973)
13. Armstrong, D. R., Perkins, P. G.: Inorg. Chim. Acta **10**, 77 (1974)
14. Armstrong, D. R., Fortune, R., Perkins, P. G.: J. Non-Crystalline Solids **24**, 313 (1977)

Received March 9, 1981